Pergamon

J. Geodynamics Vol. 19, No. 1, pp. 65–78, 1995

0264-3707/95 $7.00 + 0.00

0264-3707(94)E0002-C

ACTIVE DEFORMATION OF THE SHALLOW PART OF THE SUBDUCTING LITHOSPHERIC SLAB IN THE SOUTHERN AEGEAN

ANASTASIA A. KIRATZI and CONSTANTINOS B. PAPAZACHOS

Geophysical Laboratory, University of Thessaloniki, GR 540-06, Greece

(Received for publication 17 February 1993; accepted 1 March 1994)

Abstract—Seismic strain rates estimated from volume-averaged moment tensor data are combined with the strike, dip angle and extent of the subducting lithosphere to study the slab deformation in the shallow part (40–100 km) of the southern Aegean Wadati–Benioff zone. The upper surface of this zone has an amphitheatrical shape, strikes parallel to the sedimentary arc and dips at a low angle (14°) from the outer (convex) side to the inner (concave) side of the Hellenic arc, that is, from the eastern Mediterranean Sea to the Aegean Sea. The fault plane solutions used in the summation, indicate reverse faulting with a considerable strike-slip component and T axis plunging more steeply than the subducting lithosphere. The results show that the subducting slab is in a state of down-dip extension which occurs along the dip of Wadati–Benioff zone at a rate of about 1 cm p.a., while a fast shortening, at a rate of about 3 cm p.a., occurs parallel to the general trend of the Hellenic arc.

INTRODUCTION

The African plate is subducted under the Aegean lithosphere, along the Hellenic arc, in an amphitheatre-like shape outlined by earthquake hypocentres (Papazachos and Comninakis, 1969, 1971; McKenzie 1978; LePichon and Angelier, 1979). The seismic activity is very intense along the Hellenic arc and extends up to depths of 180 km (Comninakis and Papazachos, 1980; Hatzfeld and Martin, 1992). The dip of the zone does not seem to be constant, as there is a gently dipping zone down to about 80–100 km and then a steeper one down to 180 km (Papazachos, 1990; Hatzfeld and Martin, 1992).

In this paper, we attempt to see how the earthquake source mechanisms may constrain the strain rate and hence the rates of motion within the subducting slab. We examine the gently dipping part of the slab which is defined by the seismicity in the depth range of 40 to about 100 km. There is evidence, from the distribution of uniform moment release, that this part of the slab is coupled with the upper shallow part (Papazachos, 1990). So, we believe, that the deformation within it should be also considered in the determination of the seismic proportion of the total deformation along the Hellenic arc. Plate motion models predict the

overall motion between Africa and Eurasia to amount to about 1.0 cm p.a. convergence at Crete island (Chase 1978; DeMets *et al.*, 1990).

In previous work (Papazachos *et al.*, 1992; Kiratzi and Papazachos, 1993), it was found that along the Hellenic arc the deformation due to shallow seismicity, at depths less than 40 km, is taken up as compression at a rate that ranges from 6 to 21 mm p.a., average 12 mm p.a., in a direction of N22–31°E. Tselentis *et al.* (1988) and Jackson and McKenzie (1988a, b) have also determined deformation rates from shallow seismicity. It seems that at the Hellenic arc the larger and most significant earthquakes (M 8.0) occur at depths greater than, say, 40 km (Galanopoulos, 1965; Papazachos and Comninakis, 1971; Papazachos, 1990). For this reason, it is of interest to determine the deformation pattern of the intermediate depth seismicity.

METHOD OF ANALYSIS

The method of analysis followed here is published in Papazachos and Kiratzi (1992). The methodology is based on Kostrov's (1974), Molnar's (1979) and Jackson and McKenzie's (1988a) formulation. The reader is referred to these papers for a detail description of the procedure. However, the basic steps of the data analysis are briefly repeated in the following.

The annual scalar moment rate, $\dot{M}_o$, is calculated for each seismogenic source volume using the relations defined by Molnar (1979),

$$\dot{M}_o = \frac{A}{1-B} \cdot M_{o,\max}^{(1-B)} \tag{1}$$

where $M_{o,\max}$ is the scalar moment of the largest ever observed earthquake in the volume and

$$A = 10^{(a+(bd/c))} \quad \text{and} \quad B = \frac{b}{c} \tag{2}$$

where a and b are the constants of the Gutenberg–Richter relation and c and d are the constants of the moment magnitude realtion:

$$\log M_o = cM_s + d. \tag{3}$$

Then, for each volume we calculate the tensor, $\bar{\mathbf{F}}_{ij}$, using the following relation:

$$\bar{\mathbf{F}}_{ij} = \frac{\sum_{n=1}^{N} \mathbf{M}_{ij}^n}{N} = \frac{\sum_{n=1}^{N} M_o^n \mathbf{F}_{ij}^n}{N} \tag{4}$$

where M_o^n is the scalar moment of the nth focal mechanism, $\mathbf{F}_{ij}^n$ is a function of the strike, dip and rake of this focal mechanism (from Aki and Richards, 1980) and N is the number of the focal mechanisms available.

The equations for the strain rate tensor, $\dot{\varepsilon}_{ij}$, defined by Kostrov (1974) and the integrated rates of motion normal and parallel to the boundaries of each source volume, tensor $\mathbf{U}_{ij}$, defined by Jackson and McKenzie (1988a), are now transformed as follows:

$$\dot{\varepsilon}_{ij} = \frac{1}{2\mu V} \frac{\sum_{n=1}^{N} \mathbf{M}_{ij}}{T} = \frac{1}{2\mu V} \dot{M}_o \bar{\mathbf{F}}_{ij} \quad i,j = 1,2,3 \tag{5}$$

$$\mathbf{U}_{11} = \frac{1}{2\mu l_2 l_3} \dot{M}_o \bar{\mathbf{F}}_{11}, \qquad \mathbf{U}_{22} = \frac{1}{2\mu l_1 l_3} \dot{M}_o \bar{\mathbf{F}}_{22}, \qquad \mathbf{U}_{33} = \frac{1}{2\mu l_1 l_2} \dot{M}_o \bar{\mathbf{F}}_{33}$$

$$\mathbf{U}_{12} = \frac{1}{\mu l_1 l_2} \dot{M}_o \bar{\mathbf{F}}_{12} \tag{6}$$

$$\mathbf{U}_{23} = \frac{1}{\mu l_1 l_3} \dot{M}_o \bar{\mathbf{F}}_{23}, \qquad \mathbf{U}_{13} = \frac{1}{\mu l_1 l_3} \dot{M}_o \bar{\mathbf{F}}_{13}$$

where μ is the shear modulus ($5 * 10^{11}$ dyn/cm^2 in our case), V is the deforming volume, l_1 and l_2 is the length and the width of the volume, respectively, while l_3 denotes the thickness of the seismogenic layer. The reference system, $Ox_1x_2x_3$, used corresponds to the $Ol_1l_2l_3$ system of the zone. It is obvious that since $\bar{\mathbf{F}}_{ij}$ is calculated in the North-East-down system, from Aki and Richards (1980), a rotation of $\mathbf{F}_{ij}$ in the reference system of the zone is necessary before it is incorporated in equations (5) and (6).

ESTIMATION OF THE ERRORS

In Papazachos and Kiratzi (1992) a detailed error analysis was performed by simulating the problem using a Monte Carlo technique. The results showed that errors in the tensor $\bar{\mathbf{F}}_{ij}$ have little influence in the uncertainty of the magnitude of deformation when compared to those introduced by the seismic moment rate, $\dot{M}_o$, which are a factor of 3. Errors in $\bar{\mathbf{F}}_{ij}$, however, influence the direction of deformation where errors in $\dot{M}_o$ have no effect.

THE DATA

Earthquakes with depths in the range of 40–100 km were depicted from the catalogue of Comninakis and Papazachos (1986) for the period 1901–1985 and the monthly bulletins of the National observatory of Athens and of the Geophysical Laboratory of the University of Thessaloniki, for the period 1986–1990. The depths listed in these catalogues are taken from ISC. For the historical earthquakes (before the present century) the appropriate information was collected from Papazachos and Papazachou (1989).

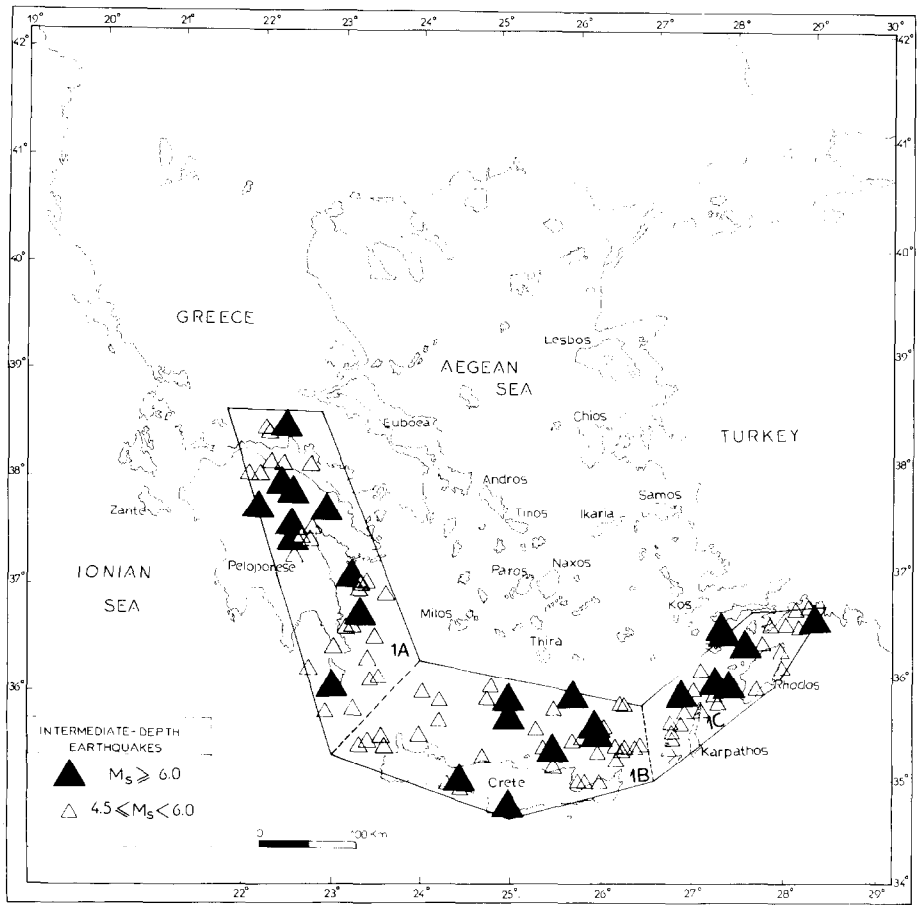

Fig. 1. The intermediate depth ($40\,km \leq h \leq 100\,km$) seismicity of the southern Aegean area, for the period 1810–1990, and the three seismogenic source volumes identified by Papazachos (1990).

Figure 1 shows the epicenters of the intermediate depth earthquakes ($40\,km \leq h \leq 100\,km$). Earthquakes with magnitude larger than 6.0 are shown with large black triangles. The area studied has been divided into three seismogenic regions (from Papazachos, 1990), as is shown in the figure, that are examined separately here. The maximum magnitude, M_{max}, (input in equation 1), in all three areas was assumed to be equal to 8.0, $M_{o,max}$ equal to 10^{28} Nm.

Table 1 gives information on the parameters used in the analysis. The length, l_1, the width, l_2, and the azimuth, ξ^o, of each source were calculated from the distribution of seismicity using a simple least squares technique (Papazachos and Kiratzi, 1992). The thickness of the seismogenic layer, l_3, that is the thickness of the Wadati–Benioff zone, was taken equal to 30 km, determined from a depth-distance cross section of recent events (to be shown later).

Table 2 gives information on the focal mechanisms of the intermediate depth earthquakes used in the moment tensor analysis. These are the focal mechanisms

that, at least we think, are the best constrained ones. It is true that there are not many recent intermediate depth earthquakes, large enough to determine their focal mechanism parameters with waveform inversion. We use fault plane solutions for a time period of about 30 yr and we hope that we sufficiently sample the largest events of the southern Aegean Wadati–Benioff zone. There were some additional fault plane solutions, though, which we decided not to include in the analysis. One Harvard solution for an event that occurred in the western part (May 29, 1987 $M = 5.4$, $h = 57$ km) was not used because it clearly showed N–S extension which indicates that this event is probably a shallow one. Also, the focal mechanism solution from Taymaz *et al.* (1990) for the event of Sept. 22, 1975 ($m_b = 5.4$, $h = 64$ km) was not used, because it showed a motion completely different from all other events in this part of the arc. We also excluded the fault plane solutions determined by Beisser *et al.* (1990), because they were based on the inversion of one-station data only. Thus, we ended up with only 12 events with quite good focal mechanisms, seven of which were determined by waveform modeling, to perform the moment tensor analysis. However, judging from the fact that we obtained rather consistent results, we believe that the geometry of the deformation would not alter dramatically even if we had a larger set of focal mechanism data.

Table 1. Information on the parameters of the seismogenic source volumes of the Aegean area

Source volume	t	M_{min}	ξ^o	M_{max}	l_1 (km)	l_2 (km)	a	b	$\dot{M}_o * 10^{20}$ (Nm p.a.)
1A Western									
36.40, 24.00	1897	7.0	159	8.0	326	107	2.00	0.5	0.15
38.70, 22.80	1911	5.5							
38.70, 21.70	1926	5.0							
35.50, 23.00	1965	4.5							
1B Central									
35.50, 23.00	1810	7.5	93	8.0	290	122	2.00	0.5	0.15
34.90, 25.00	1911	5.5							
35.20, 26.60	1926	5.0							
35.90, 26.50	1965	4.5							
36.40, 24.00									
1C Eastern									
35.20, 26.60	1863	7.5	54	8.0	196	77	1.94	0.5	0.13
36.00, 28.00	1911	5.5							
36.70, 28.60	1926	5.0							
36.70, 27.80	1965	4.5							
35.90, 26.50									

First two columns: coordinates defining the limits of the seismogenic source volume, t is the year since when the data are complete for a threshold magnitude, M_{min}, ξ^o is the azimuth of the source's principal direction with north, M_{max} is the maximum magnitude for the area, l_1, l_2 are the length and the width of each deforming volume, respectively, a, b are the parameters of the Gutenberg–Richter relation, from Papazachos (1990), the a-value is normalized for 1 year, and $\dot{M}_o$ is the seismic moment rate for each source determined from equation (1).

Table 2. Fault plane solutions of the intermediate depth earthquakes of the southern Aegean

Date	φ_N°	λ_E°	M_s	h (km)	Strike°	Dip°	Rake°	REF
1. May 23, 1961	36.6	28.5	6.4	70	270	35	115	R
2. Aug 28, 1962	37.8	22.9	6.8	95	241	51	58	M
3. Mar 31, 1965	38.6	22.4	6.8	78	286	17	60	P
4. Apr 9, 1965	34.9	24.2	6.1	51	63	76	157	T
5. Nov 28, 1965	36.1	27.4	6.0	73	350	30	162	P
6. Sept 13, 1972	38.0	22.4	6.3	75	235	76	48	K
7. Nov 28, 1977	36.1	27.8	5.8	85	103	46	24	E
8. June 15, 1979	34.8	24.2	5.6	40	150	75	70	T
9. Mar 19, 1983	35.0	25.3	5.7	67	44	51	139	T
10. May 22, 1984	36.1	22.8	5.3	73	75	66	142	H
11. June 19, 1987	36.8	28.1	5.5	60	316	54	137	E
12. Nov 21, 1992	35.9	22.5	6.0	70	196	50	16	H

R, Ritsema (1974), first motions; M, McKenzie (1972), first motions; P, Papazachos *et al.* (1991), first motions; T, Taymaz *et al.* (1990), waveform modeling; K, Karacostas (1988), first motions; E, Ekstrom and England (1989), centroid moment tensor inversion; H, CMT Harvard determination.

Figure 2 shows the fault plane solutions finally selected, which indicate reverse faulting with a considerable strike-slip component.

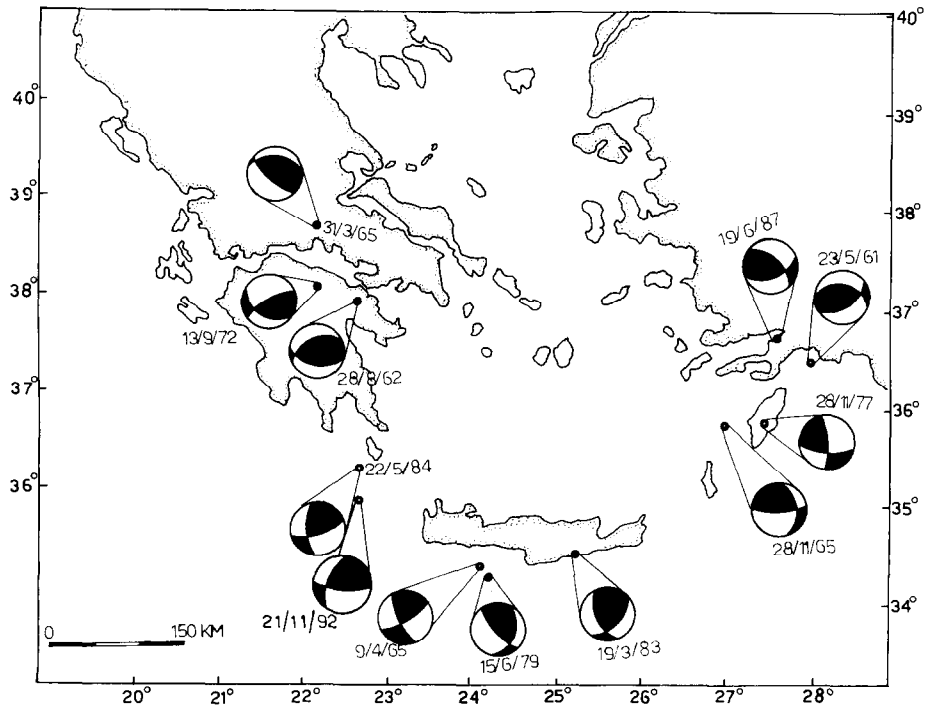

Fig. 2. Best constrained fault plane solutions for the intermediate depth (40–100 km) events of the southern Aegean area. A lower hemisphere equal area projection is used and the black quadrants denote compression while the white ones denote dilatation.

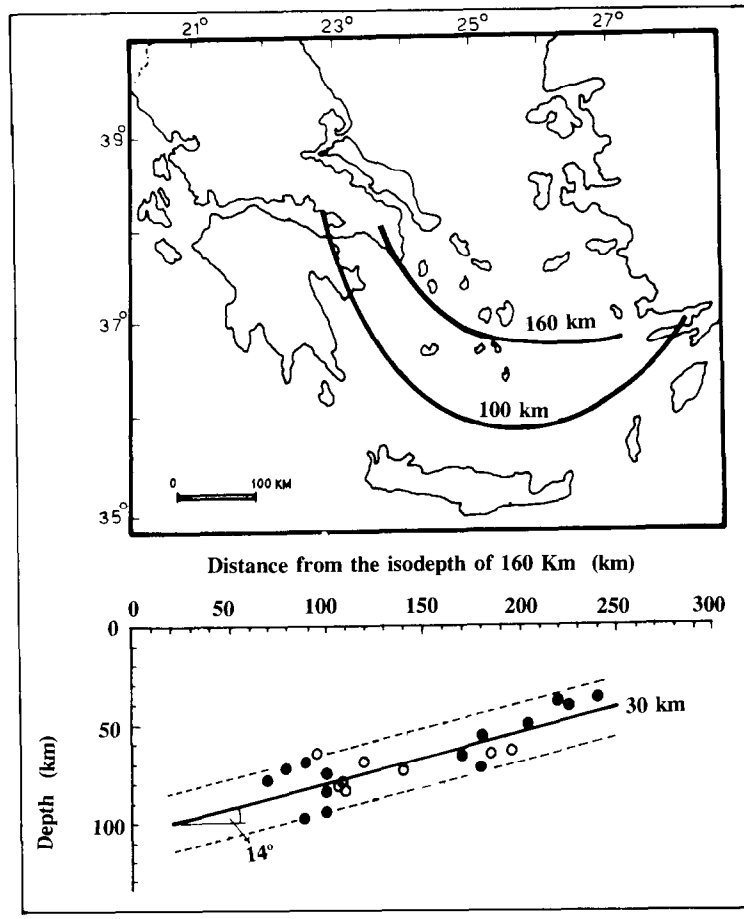

Fig. 3. Depth of intermediate depth (40–100 km) earthquakes of the period 1970–1990 vs distance from the isodepth of 160 km (shown in the upper part of the figure). (●) Denote depths calculated by waveform modeling, with a depth error of the order of 5 km (depths listed in Table 2 plus two additional values for two events whose focal mechanism we did not use), while (○) denote depths reported by ISC.

In order to calculate the scalar seismic moment of each event, in the cases where we had no direct measure of the moment, and to calculate also the values of c and d of equation (3) we used the following scaling relation:

$$\text{Log } M_o(\text{dyn.cm}) = 1.5M_s + 16.0 \tag{7}$$

which was determined from scalar seismic moments determined only by waveform modeling of intermediate depth earthquakes of the southern Hellenic arc. The slope of the line was assumed to be 1.5 (Kanamori and Anderson, 1975).

The thickness of the seismogenic layer, that is, the value of l_3, was estimated to be 30 km. In order to determine this value, we used the parameters of all the events (in the depth range 40–100 km) that occurred in the southern Aegean area after 1970 and had a magnitude greater or equal to 5.0. Figure 3 shows a cross section of the depth distribution of these events vs their distance from the

isodepth of 160 km (shown in the map in the upper part of the figure). From the same plot the mean slope of the Wadati–Benioff zone is calculated to be 14°, at this depth range (40–100 km), which was used in the calculations. Isodepths, however, show that the slope is steeper in the eastern part of the arc (Comninakis and Papazachos, 1980), but here the value of 14° was used in all three cases.

DIRECTION OF THE PRINCIPAL STRESS AXES

Using equation 4 and the data of Table 2, the six components of the tensor, $\bar{\mathbf{F}}_{ij}$, were calculated for each seismogenic source volume.

Source 1A: western

This source region lies under the eastern part of Peloponese but extends to the north up to 39° latitude and to the south up to the western corner of the island of Crete. Four fault plane solutions were used in the calculations (listed with Nos 2, 3, 6 and 10 and 12 in Table 2), and the components of the tensor, $\bar{\mathbf{F}}_{ij}$, are as follows:

−0.54	0.25	0.24
0.25	0.06	0.39
0.24	0.39	0.48

The eivenvalues of this tensor are the following:

λ	Azimuth°	Plunge°
0.80	65	55
−0.16	77	−34
−0.64	163	6

The eigenvalues are ordered such that $\lambda_1 \geq \lambda_2 \geq \lambda_3$, to represent the tensional, null and compressional axes of the equivalent double couple. Positive or negative plunge means that the vector is directed into the solid earth or above it, respectively. As was mentioned previously, the tensor $\bar{\mathbf{F}}_{ij}$ is obtained by simply summing a particular subset of moment tensors. This summation would not generally yield a double couple, with eigenvalues equal to 1, 0 and −1, but rather an arbitrary deviatoric tensor. A pure double couple would result if the orientations of the intermediate (null axes) of the individual double couples were orientated in the same direction. This would be the case for a deformation field characterized by plain strain for instance.

Source 1B: central

This source volume lies under the island of Crete. Three fault plane solutions, listed with numbers 4, 8 and 9 in Table 2 were used in the calculations. The components of the tensor, $\bar{\mathbf{F}}_{ij}$, for this source are:

0.34	0.29	0.44
0.29	−0.77	0.31
0.44	0.31	0.43

The eigenvalues of this tensor, that give the direction of the principal axes, are:

λ	Azimuth°	Plunge°
0.94	20	46
−0.06	0	−42
−0.88	100	−10

Source 1C: eastern

This source volume lies under the islands of Dodecanese (Karpathos, Rhodos, etc). Four fault plane solutions were used in the calculations, listed with Nos 1, 5, 7 and 11 in Table 2, and the components of the tensor, $\bar{\mathbf{F}}_{ij}$, for this source are as follows:

−0.51	−0.32	0.37
−0.32	−0.04	−0.35
0.37	−0.35	0.54

The eigenvalue pattern of the tensor is:

λ	Azimuth°	Plunge°
0.87	127	−57
−0.17	105	31
−0.70	21	−10

It is observed that in all three parts of the area the eigenvalue of $\bar{\mathbf{F}}_{ij}$ that corresponds to the T axis is close to 1 (0.80, 0.94 and 0.87), which indicates that the T axis, determined from the fault plane solutions of different earthquakes in each source volume, has an almost constant direction.

Figure 4 is a lower hemisphere equal area projection of the P (○) and T (●) axes of the fault plane solutions shown in Table 1, for the three seismogenic source volumes. It is clear that the T axes are less variable than the P axes are. They are directed, in all three source volumes, from the convex (eastern Mediterranean) to the concave (Aegean) part of the arc and dip at a considerably steeper angle than the dip of the slab (55°, 46° and 57° from west to east). A steep dip of the T axes has been also noted before (Papazachos *et al.*, 1991). The P axes appear to be more variable, and are almost horizontal (6°–10°) which indicates that they lie within the shallow dipping slab.

SEISMIC STRAIN RATES

Following the method described above we calculated the strain rate tensor, $\dot{\epsilon}_{ij}$, and the velocity tensor, U_{ij}, for each seismogenic source volume, using equations (5) and (6). The results are summarized in Table 3.

The maximum strain rate release changes from west towards east from $6.9*10^{-8}$ p.a. to $8.1*10^{-8}$ p.a. to $16.0*10^{-8}$ p.a., which, except for the eastern part, is about a factor of 2 smaller than the maximum strain rate release observed for the shallow seismicity in the Aegean area (Kiratzi and Papazachos, 1993). From the results of Table 3 it is indicated that compression occurs parallel to the strike of the arc in all three seismogenic volumes at a rate of 29 mm p.a. in the western part and of 34 mm p.a. both in the central and the eastern parts. This compression takes place at a shallow angle, within the subducting lithosphere. Approximately down dip extension occurs normal to the strike of the Hellenic arc, at a rate of 8 mm p.a. in the western part, 14 mm p.a. in the central and 17 mm p.a. in the eastern part. Moreover, in the eastern part of the Hellenic arc the dip of the vector of the maximum extension (~44°) is considerably larger than the mean dip of the shallow part of the Wadati–Benioff zone (14°).

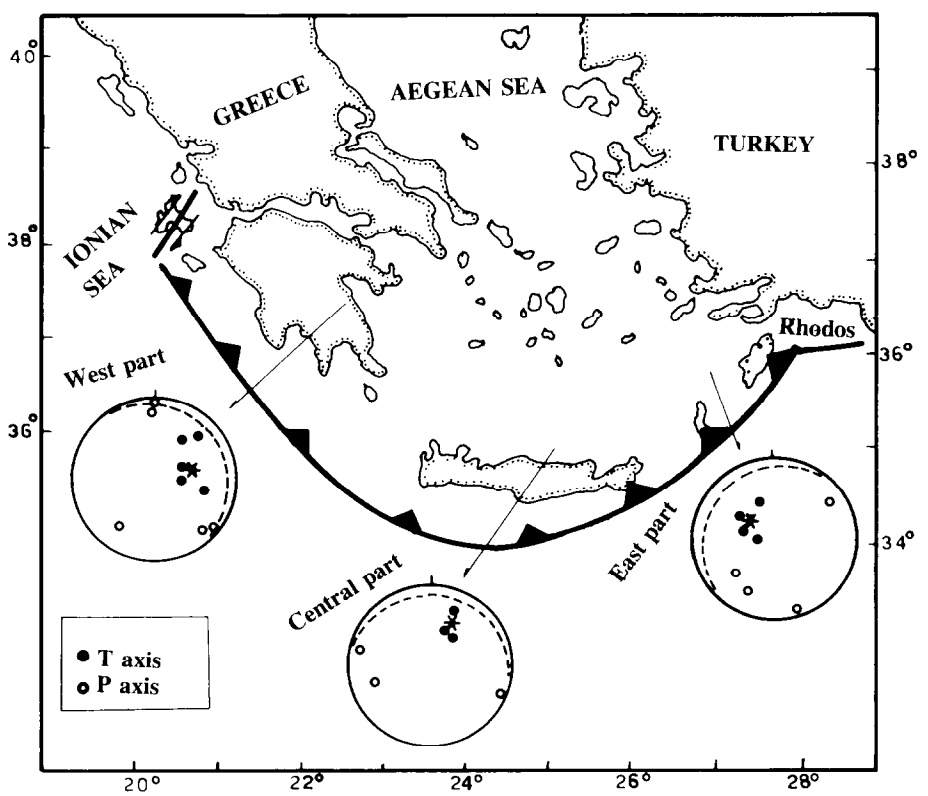

Fig. 4. Lower hemisphere equal area projection of the P (○) and of the T axes (●) of the fault plane solutions, shown in Fig. 2, for each source volume separately. The asterisks (*) show the T axis obtained from the eigenvalues of tensor $\bar{F}_{ij}$, and (----) shows the orientation of the Wadati–Benioff zone, in each case.

Table 3. Seismic strain rates (*10 ^{8}/a) and seismic deformation velocities (in mm/p.a.) for each source volume

Source 1A							
Strain rate (*10^{-8} p.a.)				$\dot{\varepsilon}_{11}$	$\dot{\varepsilon}_{12}$	$\dot{\varepsilon}_{13}$	$\dot{\varepsilon}_{22}$	$\dot{\varepsilon}_{23}$	$\dot{\varepsilon}_{33}$
(1:north, 2:east, 3:down)				−6.85	5.46	2.16	6.12	5.11	0.72
Seismic deformation velocity				U_{11}	U_{22}	U_{13}	U_{22}	U_{23}	U_{33}
(1:north, 2;east, 3:down)				−23.87	11.81	−0.83	2.87	3.01	−0.58
Eigenvalues of U_{ij}:	λ_1	λ_2	λ_3 (in mm p.a.)						
	−28.46	0.81	−0.12						
Azimuth°	159	70	56						
Plunge°	−4	16	−73						
Seismic deformation velocity				U_{11}	U_{22}	U_{13}	U_{22}	U_{23}	U_{33}
(1:159°SE, 2:249°SW dip −14°, 3:249°SW dip 76°, the zone system).				−28.45	0.26	−0.67	5.83	−3.97	1.03
Source 1B									
Strain rate (*10^{-8} p.a.)				$\dot{\varepsilon}_{11}$	$\dot{\varepsilon}_{12}$	$\dot{\varepsilon}_{13}$	$\dot{\varepsilon}_{22}$	$\dot{\varepsilon}_{23}$	$\dot{\varepsilon}_{33}$
(1:north, 2:east, 3:down)				7.58	6.16	4.23	−8.13	6.12	0.55
Seismic deformation velocity				U_{11}	U_{22}	U_{13}	U_{22}	U_{23}	U_{33}
(1:north, 2:east, 3:down)				8.95	12.59	0.32	−27.83	9.18	−1.92
Eigenvalues of U_{ij}:	λ_1	λ_2	λ_3 (in mm p.a.)						
	−34.08	13.51	−0.22						
Azimuth°	106	20	147						
Plunge°	−15	12	70						
Source 1C									
Strain rate (*10 ^{8} p.a.)				$\dot{\varepsilon}_{11}$	$\dot{\varepsilon}_{12}$	$\dot{\varepsilon}_{13}$	$\dot{\varepsilon}_{22}$	$\dot{\varepsilon}_{23}$	$\dot{\varepsilon}_{33}$
(1:north, 2:east, 3:down)				−9.40	−8.98	16.00	−2.27	−6.83	11.67
Seismic deformation velocity				U_{11}	U_{22}	U_{13}	U_{22}	U_{23}	U_{33}
(1:north, 2:east, 3:down)				−20.07	−17.51	12.63	−4.76	−3.82	4.64
Eigenvalues of U_{ij}:	λ_1	λ_2	λ_3 (in mm p.a.)						
	−33.53	16.53	−3.18						
Azimuth°	30	133	107						
Plunge°	−13	−44	43						
Seismic deformation velocity				U_{11}	U_{22}	U_{13}	U_{22}	U_{23}	U_{33}
(1:54°NE, 2:144°SE dip −14°, 3:144°SE dip 76°, the zone system).				−27.57	14.59	0.20	5.09	−9.76	2.30

Isodepths (Fig. 3), however, show that the dip of the zone is also larger in the eastern part of the arc.

DISCUSSION AND CONCLUSIONS

We examined the deformation caused by the earthquakes that occur in the intermediate part of the Wadati–Benioff zone (40–100 km) along the Hellenic arc, on the basis of seismicity and moment tensor data. At this depth range, the Wadati–Benioff zone dips to the inner (concave) side of the Hellenic arc at a low angle (~14°). it is believed that in this depth range coupling occurs between the subducted oceanic lithospheric slab and the overriding Aegean lithosphere (Papazachos, 1990), and we thought the contribution of these intermediate depth events to the deformation of the Hellenic arc should be also considered.

Figure 5 is a graphic illustration of the maximum relative velocities, as these are obtained from the eigensystem of the tensor, U_{ij}. A lower hemisphere equal

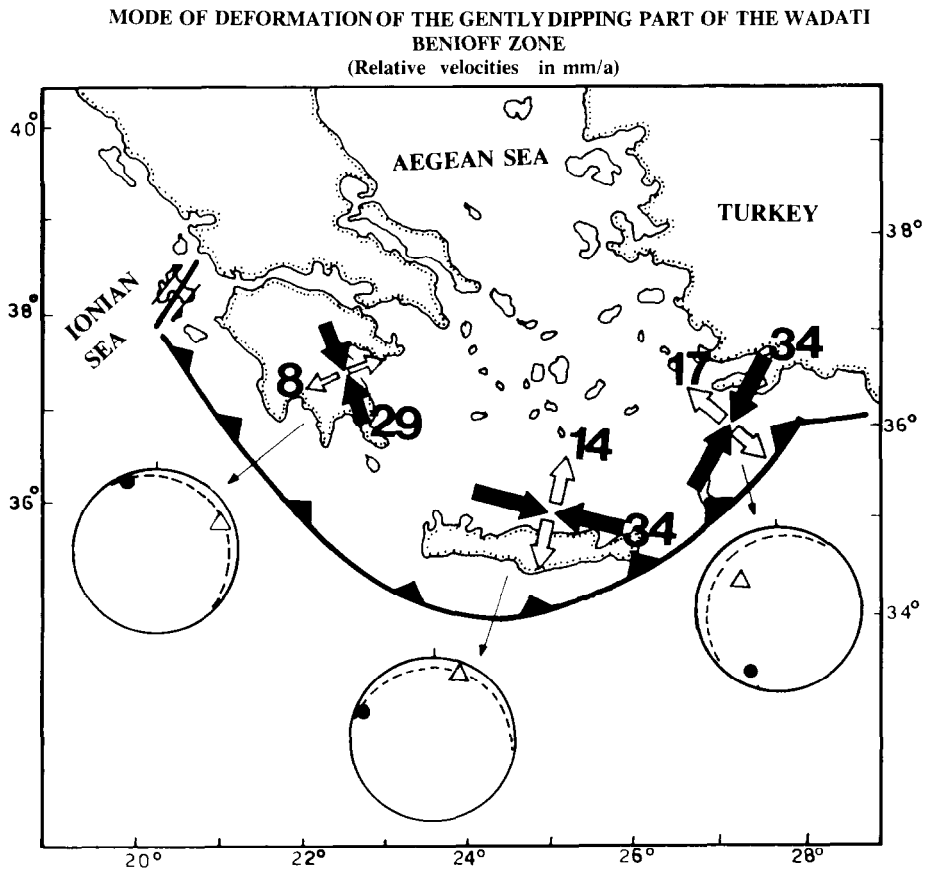

Fig. 5. Graphic illustration of the maximum relative velocities (derived from the eigensystem of tensor U_{ij}), for the shallow part (40–100 km) of the Wadati–Benioff zone. Converging arrows denote compression, while diverging arrows denote extension (numbers next to the arrows give the velocities in mm p.a.). The large circles show a lower hemisphere equal area projection of the direction of the maximum extensional velocity (△) and of the maximum shortening velocity (●) for each source. The dashed line shows the approximate orientation of the Wadati–Benioff zone.

area projection of the direction of the maximum extension (△) and of the maximum shortening (●) is also shown in the figure. The subducting slab, at the depths of 40–100 km, is in a state of down-dip tension which seems to increase from west to east (8 mm p.a. in the west, 14 mm p.a. in the central and 17 mm p.a. in the east). It seems more reasonable, though, to consider the average value, 13 mm p.a., since these values are within error limits (Papazachos and Kiratzi, 1992). Nearly horizontal compression along the strike of the Hellenic arc is observed, at an average rate of 32 mm p.a. This compression was also observed by Taymaz *et al.* (1990). They interpreted it as the possible effect of the eastern Mediterranean to be in a state of E–W compression from processes unrelated to the subduction. As a matter of fact, the component of seismic extension could be easily attributed to slab pull-forces acting on the subducting lithosphere but the component of the compression, of about

3 cm p.a., is more difficult to explain. The T axes of the intermediate depth events (40–100 km) are the less variable and dip to the inner side of the Hellenic arc at generally steeper angles than the slab dip. However, the orientation of the relative velocity vectors indicate deformation within the subducting lithosphere.

In previous work (Papazachos *et al.*, 1992; Kiratzi and Papazachos, 1993) it was found that the shallow seismicity along the convex side of the Hellenic arc can account for about 12 mm p.a. of nearly horizontal seismic shortening due to slip on low angle thrust faults. According to the results of the present paper, in the shallow dipping part of the Wadati–Benioff zone, horizontal seismic shortening of 32 mm p.a. parallel to its strike (and to the strike of the arc) combined with seismic extension of 13 mm p.a. along its dip produces reverse motion with considerable strike-slip component. It is interesting to note that the amount of compression (12 mm p.a.) along the convex side of the arc and of extension (13 mm p.a.) observed at the shallow dipping part of the Wadati–Benioff zone are nearly the same, both in magnitude and in direction.

Acknowledgement—The authors would like to express their sincere gratitude to Professor Basil Papazachos, director of the Geophysical Laboratory of the University of Thessaloniki, for his encouragement, guidance and helpful suggestions throughout this work.

REFERENCES

Aki K. and Richards P. (1980) *Quantitative Seismology: Theory and Methods*, 557 pp. Freeman, San Francisco, CA.

Beisser M., Wyss M. and Kind R. (1990) Inversion of source parameters for subcrustal earthquakes in the Hellenic Arc. *Geophys. J. Int.* **103**, 439–450.

Chase P. (1978) Plate kinematics: the Americas, east Africa and the rest of the world. *Earth and Planet. Sci. Lett.* **37**, 355–368.

Comninakis P. and Papazachos B. (1980) Space and time distribution of the intermediate focal depth earthquakes in the Hellenic arc. *Tectonophysics* **70**, 135–147.

Comninakis P. and Papazachos B. (1986) A catalogue of earthquakes in the Aegean and surrounding area for the period 1901–1985. *Publ. of the Geophys. Lab., Univ. of Thessaloniki* **1**, 167 pp.

DeMets C., Gordon R., Argus D. and Stein S. (1990) Current plate motions. *Geophys. J. Int.* **101**, 425–478.

Ekstrom G. and England P. (1989) Seismic strain rates in regions of distributed continental deformation. *J. Geophys. Res.* **94**, 10231–10257.

Galanopoulos A. (1965) On mapping of the seismic activity in Greece. *Ann. Geofis.* **16**(1), 306–312.

Hatzfeld D. and Martin C. (1992) Intermediate depth seismicity in the Aegean defined by teleseismic data. *Earth and Planet. Sci. Lett.* **113**, 267–275.

Jackson J. and Mckenzie D. (1988a) The relationship between plate motions and seismic moment tensors, and the rates of active deformation in the Mediterranean and Middle East. *Geophysical Journal Int.* **93**, 45–73.

Jackson J. and McKenzie D. (1988b) Rates of active deformation in the Aegean Sea and surrounding regions. *Basin Res.* **1**, 121–128.

Kanamori H. and Anderson D. (1975) Theoretical basis for some empirical relations in seismology. *Bull. Seism. Soc. Am.* **65**, 1073–1095.

Karakostas B. (1988) Fault plane solutions of the earthquakes of the Aegean and the surrounding area. *Proc. of the 1st Symposium on the Recent Trends in Seismology and Geophysics, Thessaloniki, July 1–3, 1988* pp. 1–8.

Kiratzi A. and Papazachos C. (1993) Coseimic crustal deformation from the Azores triple junction to Middle East. *Publ. of the Geophys. Lab.* **21**, 20.

Kostrov V. (1974) Seismic moment and energy of earthquakes, and seismic flow of rock. *Izv. Acad. Sci. USSR Phys. Solid Earth* **1**, 23–44.

LePichon X. and Angelier J. (1979) The Hellenic arc and trench system: a key to the neotectonic evolution of the eastern Mediterranean area. *Tectonophysics* **60**, 1–42.

McKenzie D (1972) Active tectonics of the Mediterranean region, *Geophys. J. R. astr. Soc.* **30**, 109–185.

McKenzie D. (1978) Active tectonics of the Alpine–Himalayan belt: the Aegean Sea and surrounding regions. *Geophys. J. R. astr. Soc.* **55**, 217–254.

Molnar P. (1979) Earthquake recurrence intervals and plate tectonics. *Bull. Seism. Soc. Am.* **69**, 115–133.

Papazachos B. (1990) Seismicity of the Aegean and surrounding area. *Tectonophysics* **178**, 287–308.

Papazachos B. and Comninakis P. (1969) Geophysical features of the Greek island arc and eastern Mediterranean ridge. *C.R. Seances de la Conference Reunie a Madrid* **16**, 74–75.

Papazachos B. and Comninakis P. (1971) Geophysical and tectonic features of the Aegean arc. *J. Geophys. Res.* **76**, 8517–8533.

Papazachos B. and Papazachou C. (1989) *The Earthquakes of Greece*. Ziti Publication Company, Thessaloniki, 356 pp.

Papazachos B., Kiratzi A. and Papadimitriou E. (1991) Fault plane solutions for earthquakes in the Aegean area. *Pageoph.* **136**, 405–420.

Papazachos C. and Kiratzi A. (1992) A formulation for reliable estimation of active crustal deformation and its application to central Greece. *Geophys. J. Int.* **111**, 424–432.

Papazachos C., Kiratzi A. and Papazachos B. (1992) Rates of active crustal deformation in the Aegean and the surrounding area. *J. Geodynamics* **16**, 147–179.

Ritsema A. (1974) The earthquake mechanisms of the Balkan region. *R. Netherl. Meteorol. Inst., De Bilt, Sci. Rep.* 74–4.

Taymaz T., Jackson J. and Westaway R. (1990) Earthquake mechanisms in the Hellenic Trench near Crete. *Geophys. J. Int.* **102**, 695–731.

Tselentis G., Stavrakakis G., Makropoulos K., Latousakis J. and Drakopoulos J. (1988) Seismic moments of earthquakes at the western Hellenic arc and their application to the seismic hazard of the area. *Tectonophysics* **148**, 73–82.